Journal of Metals, Materials and Minerals, Vol. 30, No. 2, pp. 58-66, 2020

Effect of polystyrene molecular weight and zinc oxide concentration on dewetting behavior of polymeric thin films

Kattaleeya SUJAROON[1], Phanawan WHANGDEE[2], and Nampueng PANGPAIBOON[1,*]

[1] *Department of Industrial Physics and Medical Instrumentation, Faculty of Applied Science, King Mongkut's University of Technology North Bangkok, Bangkok, 10800, Thailand*
[2] *Department of Applied Physics, Faculty of Sciences and Liberal Arts, Rajamangala University of Technology Isan, Nakhon Ratchasima, 30000, Thailand*

[*]**Corresponding author e-mail:** nampueng.p@sci.kmutnb.ac.th

Received date:
30 September 2019
Revised date:
10 March 2020
Accepted date:
21 March 2020

Keywords:
Polystyrene thin films
ZnO nanoparticles
Dewetting behavior

Abstract

The separation between ultra-thin polymer film on metal oxide substrate is called dewetting. Dewetting causes the polymer films to loss their stability and other important properties, for example, the films may short circuit or reduce their transparency. Therefore, the stability of polymer thin films on substrate need to be improved. Addition of nanoparticles is one of the most popular technique used to increase the stability of polymer thin films. The correlation between the different of molecular weight and ZnO concentration on dewetting behavior was studied in this research. The appropriate concentration of ZnO on dewetting suppression in each molecular weight was examined. Furthermore, the variation of dewetting pattern in each molecular weight system was analyzed. In this research, PS (13K and 30K) solutions mixed with ZnO suspension in toluene were prepared. The concentrations of ZnO in PS solution were 0-1.0 wt%. All composite thin films were coated by spin-casting technique and annealed at a temperature of 100°C in a vacuum oven to induce dewetting behavior. The topographies of annealed thin films were studied by using Optical microscope (OM) and Scanning electron microscope (SEM). The thicknesses of thin films were examined by Atomic force microscope (AFM). The surface energies of PS and PS-ZnO composite films were measured and calculated by using contact angle measurement. From the results, we found that addition of ZnO nanoparticles at concentrations 0.7 and 1.0 wt% are the optimum concentration for dewetting inhibition of PS13K and PS30K films, respectively.

1. Introduction

Polymer thin film is a film with a thickness of less than 100 nm. Naturally, thin polymer film coated on metal-oxide substrate is not stable [1-5]. Polymer thin film and metal oxide substrate are different material causing a separation at an interface and hole creation, this phenomenon is called dewetting [6]. Dewetting behavior is a significant problem for thin film usage in industry because when dewetting occurs, the films lose their stability and essential properties, such as insulation and transparency. The stages of dewetting behavior can be divided into 3 stages: early stage, intermediated stage, and final stage or completely dewet [7].

Many researchers have studied the inhibition of dewetting behavior of polymer thin film [8]. There are 3 common methods to inhibit dewetting: interface modification [9-11], polymer modification [12], and polymer cross-linking [13-14]. In the last decade, the new simple method to prevent dewetting behavior occurs, addition of nanoparticles [15-19]. Barnes *et al.* [20] is the first investigator who found that addition small amount of C_{60} (fullerene) nanoparticles can suppress dewetting behavior. In their research, the inhibition caused by C60 nanoparticles in polymer matrix migrate to the interface between polystyrene film and substrate. After that, in recent years, the addition of various nanoparticle into polymer thin film as an additive for dewetting inhibition have been studied, such as Ag [21], TiO_2 [22] and ZnO [23-25].

In 2015, Roy *et al.* [19] discussed the effect of surface energy on the movement of nanoparticles for dewetting suppression. The stable location of nanoparticles depends on concentration of nanoparticles which can be divided into 3 regimes. In their research, surface energy of substrate, surface energy of nanoparticles, and concentration of nanoparticle are the three important parameters to select the mechanism for inhibition dewetting behavior of polymer thin film [8].

ZnO is one of the materials used to add into polymer film as a pH sensing [26], antibacterial agents [27] and antimicrobial agents [28]. These studies confirm that ZnO has an ability to mix with polymer films. ZnO is an interesting material due to the fact that it is non-toxic, has high chemical stability, and has low cost. Our research group has studied the effect of the ZnO concentrations on dewetting suppression in polystyrene (PS) film, recently [24-25]. From the researches, we found that ZnO nanoparticles showed their ability to suppress dewetting in PS thin film. Pinning contact

DOI: 10.14456/jmmm.2020.21

line effect was expected as a major role of the inhibition. However, the various ZnO concentration and film thickness effect dewetting inhibition property. Small amounts of ZnO in PS film can suppress dewetting, while higher ZnO concentration may induce dewetting. Therefore, the suitable ZnO concentration in each PS system is required for stabilize PS thin film. Polymer molecular weight is an important factor affect thin film characteristic. To full fit discovering the dewetting inhibition knowledge, the relationship between polymer molecular weight and additive concentration should be studied. Moreover, because of chain size difference, the dewetting pattern of composite film is very attractive for material fieldwork.

In this research, we were interested in the effect of PS molecular weight and concentration of ZnO nanoparticles on the thermal stability of thin film. The shorten polymer chain were used in this study to compare with the previous research. Generally, polymer molecular weight indicates a mobility of polymer thin film. Base on the pinning contact line effect, we assume that, the movement of PS chain will affect an ability of nanoparticle pressing. Therefore, the fit concentrations of ZnO added in two different PS molecular weights to increase film stability have been investigated. Dewetting pattern of all PS-ZnO thin films were observed by Optical microscope (OM) and Scanning electron microscope (SEM). Moreover, the dewetting areas of each PS-ZnO systems at all annealing conditions were calculated.

2. Experiment

2.1 Materials

Polystyrene (PS13K, M_w = 13,000 g/mol, M_w/M_n = 1.06 and PS30K, M_w = 30,000 g/mol, M_w/M_n = 1.06) was purchased from Alfa Aesar. The ZnO nanoparticles (ZnO, diameter ≤ 50 nm) that were used were agricultural grade. Toluene was used as solvent and was purchased from Fisher Chemical. Silicon wafers 1×1 cm^2 were used as substrate and were cleaned by soaking in piranha acid (H_2SO_4 70% and H_2O_2 30%) at temperature of 80°C for 1 h to remove organic compounds on the surface. After that, the silicon wafers were rinsed with DI water and dried by nitrogen gas. All silicon wafers were checked up on their cleanness by OM before using.

2.2 Preparation of PS-ZnO films

A solution of PS in toluene solvent was prepared by mixing PS at 0.5 wt% in toluene. A suspension of ZnO nanoparticle in toluene was also prepared by mixing ZnO 0.5 wt% in toluene. After that, the ZnO suspension was dropped into the PS solution to produce the composite solutions at concentrations of 0, 0.5, 0.7, and 1.0 wt%. The mixing PS-ZnO solutions were called PS13K, PS13K-ZnO0.5, PS13K-ZnO0.7 and PS13K-ZnO1.0, for PS13K system, and were called PS30K, PS30K-ZnO0.5, PS30K-ZnO0.7 and PS30K-ZnO1.0, for PS30K system. All of PS-ZnO composite solutions were homogenized by ultrasonicate bath for 5 min. Droplet of 0.2 ml PS-ZnO solution, in all conditions, was dropped and coated on a silicon wafer by spin-casting technique (MTI, VTC-100). Spinning rate was 1000 rpm for 10 seconds. PS-ZnO films were dried at room temperature for 24 h.

2.3 Characterization of PS-ZnO films

The surface energies of as-cast films were calculated by using contact angle measurement between 2 types of liquids, DI water and diiodomethane, combined using Owens and Wendt's equation as shown in Equation 1 [29]. In Equation 1, γ is surface energy, subscript S, L and V are solid, liquid and vapor, superscript d and h are polar and non-polar, and θ is the contact angle of DI water and diiodomethane.

$$\gamma_{LV}(1+\cos\theta) = 2\left(\sqrt{\gamma^{d}_{SV}\gamma^{d}_{LV}} + \sqrt{\gamma^{h}_{SV}\gamma^{h}_{LV}}\right) \quad (1)$$

Thickness of PS thin film was examined using atomic force microscope (VEECO, DI 3000). The surface of PS thin film was scratched by a needle. After that, the depth profiles of the scratches were measured, and the thickness was examined. From AFM analysis, the thickness of PS films at concentrations 0.5 wt% in toluene is 28.32 ± 0.6 nm.

The PS-ZnO composite films on the silicon wafer substrates were then annealed in a vacuum oven (Binder, VD 23) at a temperature of 100°C under pressure of 5 mbar for various times, 0-288 h. The surface morphologies of all PS-ZnO composite films were observed by using an optical microscope (Olympus, CX31) at 500 and 1000X magnification. At lease, three images per sample were taken for average the dewetting area. A local topography of PS-ZnO surface were observed by SEM (FEI, Quanta 250) at 10000X magnification. Dewetting areas comparing with annealing time were analyzed by using the OM images and an image analysis program. Percentages of the dewetting area were calculated by using Equation 2.

$$\%\ \text{dewetting} = \frac{\text{dewetting area}}{\text{total area}} \times 100 \quad (2)$$

3. Results and discussion

3.1 PS13K-ZnO films

In this part, the system of PS13K thin films at different concentrations of ZnO nanoparticles, 0, 0.5, 0.7, and 1.0 wt% are studied. Annealing the films at 100°C in vacuum oven for various times causes the films to become dewet. Figure 1 shows optical microscope images of annealed PS13K-ZnO composite films. From OM images, all as-cast films have smooth

and homogeneous surfaces. After annealing for 6 h, many small holes appear on the surface of the films except the PS13K-ZnO0.7. Increasing annealing time to 36 h expands the small holes, dewetting area of pure PS13K and PS13K-ZnO composite films increase. However, the film with 0.7 wt% of ZnO presents smaller holes comparing with the other conditions. Dewetting area increases almost to 100% in pure PS13K when annealing time is increased to 144 h, while the composite films show the dewetting prevention by ZnO nanoparticle. Though the expanded holes in PS13K-ZnO0.5 and PS13K-ZnO1.0 cover about 70% of film surface, dewetting area of PS13K-ZnO0.7 film is less than 40%. From the results, we confirm that addition of ZnO nanoparticles into PS13K films can inhibit dewetting behavior. Moreover, the concentration of ZnO nanoparticles at 0.7 wt% is the appropriate concentration for dewetting inhibition of PS13K films.

As we expected, the mechanism that ZnO nanoparticles use to inhibit dewetting behavior is the pinning contact line effect. This phenomenon may be confirmed by observation of the holes shape. In pure PS13K film, most of holes are circular shape. Conversely, PS13K-ZnO composite films show flower-liked shape holes. The reason of the different shape of holes is that the addition of nanoparticles into polymer films will make the nanoparticles pin the polymer chain. For PS13K system, which has low molecular weight, short-polymer chain, and high mobility, the films are easy and free movement. When the polymer chains are pressed by the nanoparticles, polymer will move and expand to the gap between ZnO. Therefore, a hole shape of composite films is look like a flower. [15].

Because of the limitation of the optical microscope, a local topography area of the films is not clearly observed. Scanning electron microscope is used to study the delicate topography of all PS13K films, as shown in Figure 2. SEM images shows the surface of PS13K-ZnO composite films at concentration 0, 0.7, and 1.0 wt% after annealed at 100°C for 72 h. From the images, we found that, in higher magnification view, PS13K-ZnO0.7 still be the optimum concentration to inhibit of dewetting behaviour as same as from OM results.

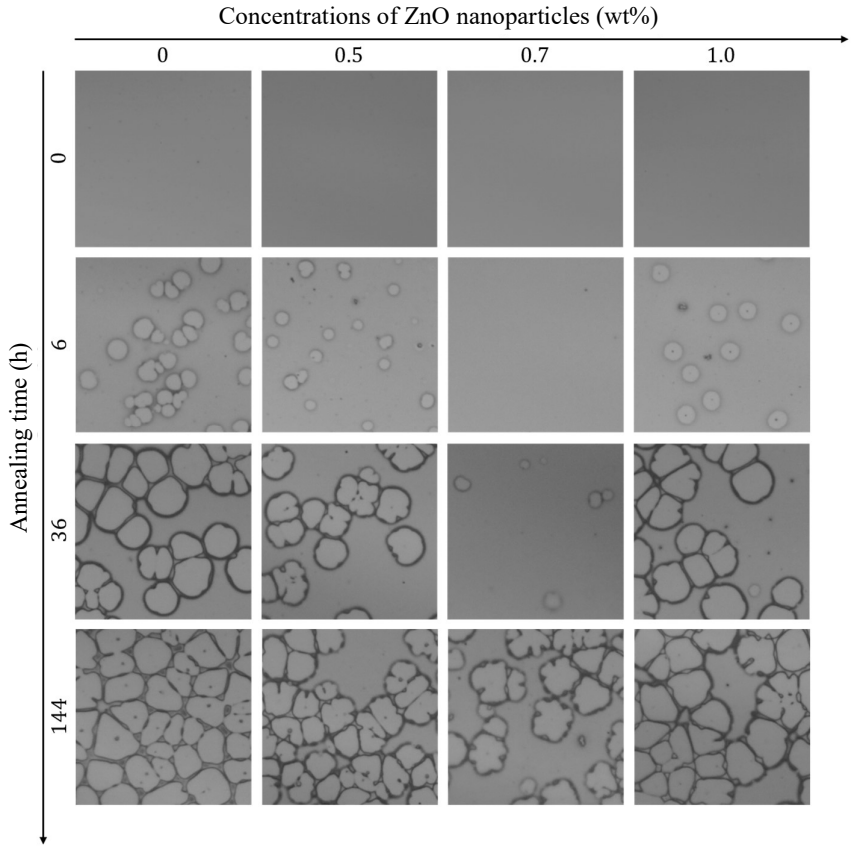

Figure 1. Optical microscope images of PS13K-ZnO films containing different concentrations of ZnO at 0, 0.5, 0.7, and 1.0 wt%, annealed temperature at 100°C for various time (magnification 1000X).

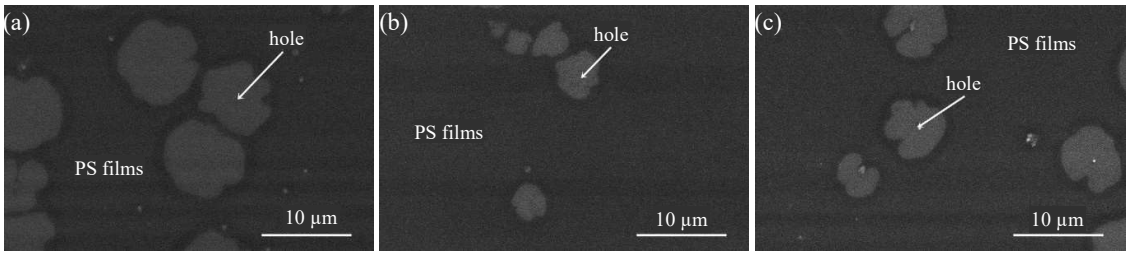

Figure 2. Scanning electron microscope images of PS13K-ZnO films, annealing temperature of 100°C for 72 h, (a) PS13K, (b) PS13K-ZnO0.7, and (c) PS13K-ZnO1.0 (magnification 10000X).

From OM images in Figure 1, we calculate the percentage of dewetting area of PS13K films system, and the results are shown as a graph in Figure 3.

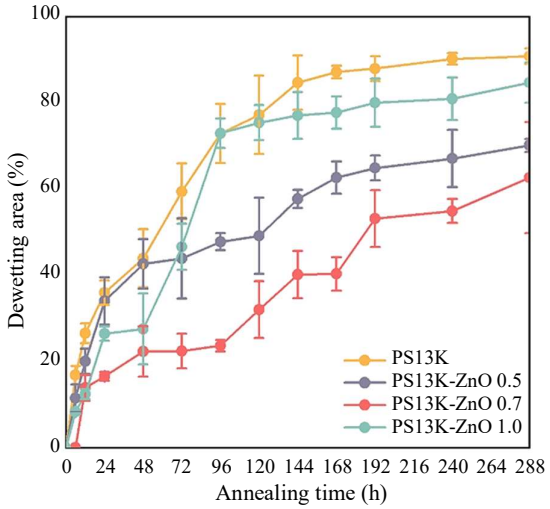

Figure 3. Percentage of dewetting area and annealing time of PS13K-ZnO films with concentrations 0, 0.5, 0.7, and 1.0 wt%.

Percentage of dewetting area of all as-cast films are 0%. After annealing for 6 h, dewetting area of all films increase. The dewetting areas of the composite films at concentrations 0, 0.5, and 1.0 wt% are 16.876%, 11.512%, and 8.295%, respectively, while PS13K-ZnO0.7 composite film shows no dewetting area occur on the surface. Increasing annealing time to 36 h, the percentage of dewetting area of all films increase to 39.591%, 40.995%, 21.776%, and 27.555% for concentrations of ZnO 0, 0.5, 0.7, and 1.0 wt%, respectively. The dewetting area of pure PS13K film increases to 90.876% when annealing time go to 288 h. Conversely, for PS13K-ZnO0.5 and PS13K- ZnO1.0 films, the percentages are 70.170% and 84.732%. Furthermore, the dewetting area of PS13K-ZnO0.7 composite films is only 62.657% at the same condition. From the results, we can approve that the dewetting area increase when increasing annealing time and the dewetting area of PS13K-ZnO0.7 is less when comparing with the others. In addition, when we focus on the dewetting rate by observing the slope of the graph, pure PS film exhibits the highest slope and PS13K-ZnO0.7 exhibits the lowest one. We can conclude that the addition of ZnO nanoparticles is not sufficient to completely prevent dewetting behavior but is able to slow the rate of hole growth.

From the results, the dewetting behavior of pure PS13K occurs after annealing for 3 h and finally become completely dewet when time go to 288 h. PS13K-ZnO0.5 and PS13K-ZnO1.0 films also start dewetting after annealing for 3 h. However, addition of ZnO nanoparticles less than 1.0 wt% show the ability to retard dewetting at the parallel annealing process. PS13K-ZnO0.7 film presents the slowest rate of dewetting. The film is initiated dewetting holes when heating up to 12 h. And finally, the film is protected for complete dewetting until 288 h and shows about 40% higher performance to inhibit dewetting comparing with pure PS13K.

3.2 PS30K-ZnO films

For higher molecular weight system, PS with molecular weight of 30,000 g/mol (PS30K) is used as polymer matrix. PS30K-ZnO composite thin films at different concentrations of ZnO nanoparticles 0, 0.5, 0.7, and 1.0 wt% are prepared. Annealing the films at 100°C in a vacuum oven for various times causes the films to become dewet, which is the same method used for the PS13K system. As-cast films have smooth and homogeneous surface as shown by OM images in Figure 4. Annealing for 6 h induces dewetting behavior. Many small holes are detected on the surfaces of pure PS30K, PS30K-ZnO0.5, and PS30K-ZnO0.7 films. Conversely, PS30K-ZnO1.0 films still maintain the smooth surface against dewetting at the same annealing time. There is no hole observed in the films. After increasing annealing time to 72 h, pure PS30K, PS30K-ZnO0.5, and PS30K-ZnO0.7 show the holes growth and dewetting area increasing, while PS30K-ZnO1.0 presents a few tiny dewetting holes. When annealing time is increased to 288 h, the holes in PS30K film are expanded, they connect with each other and nearly cover the whole surface as in the intermediate stage of dewetting. On the other hand, the size of holes in PS30K-ZnO films are still the same, all composite films show strong inhibition of dewetting. Size and number of holes are almost constant during 72-288 h of heating. The results

obviously exhibit that ZnO nanoparticles can prevent dewetting behavior of PS30K system, and the best concentrations is 1.0 wt%. The addition of ZnO nanoparticles can inhibit dewetting behavior in PS30K as well as in PS13K.

From OM images, the holes of all PS30K films are circular which is different from in PS13K. Since higher molecular weight, long-polymer chain, and low mobility, PS30K films are difficult to move. When we activate dewetting behavior by heat, and the polymer chains are pressed by the nanoparticles, the long and restricted movement of polymer chain cannot move freely. However, the polymers need to release annealing stress in the films, which means that instead of hole expansion, they create a new hole. Therefore, the shape of holes in PS30K-ZnO films are circular, and we can detect some small holes created in the composite films after annealing for a long time which cannot be observed in PS13K-ZnO.

The SEM is also used to study the local surface topography of the PS30K system. SEM images present the surface of PS30K, PS30K-ZnO0.7, and PS30K-ZnO1.0 after annealing at 100°C for 72 h, as shown in Figure 5(a), 5(b) and 5(c), respectively. From the images, at high magnification, even though all composite films can prevent dewetting, the PS30K-ZnO1.0 is the optimum concentration to inhibit of dewetting behavior. These results agree with the previous OM images.

From OM images in Figure 4, we calculate the percentage of dewetting area of all PS30K films. A graph representing the percentage of dewetting area versus annealing time is shown in Figure 6. All as-cast PS30K films present 0% of dewetting area. After annealing at temperature 100°C for 6 h, percentage of dewetting area of PS30K, PS30K-ZnO0.5, and PS30K-ZnO0.7 are increased, which are 16.824%, 4.208%, and 1.060%, respectively while there is no dewetting area that occurs in PS30K-ZnO1.0 film. Increasing annealing time to 72 h, the percentages of dewetting area of all films are increased. Pure PS30K, PS30K-ZnO0.5, PS30K-ZnO0.7, and PS30K-ZnO1.0 present dewetting area at 41.905%, 16.452%, 7.544%, and 2.221%, respectively. The dewetting area of pure PS30K films increases to 54.533% when annealing time go to 288 h. Conversely, the percentage of dewetting area of PS30K-ZnO0.5, PS30K-ZnO0.7, and PS30K-ZnO1.0 are 28.071%, 7.363%, and 2.803%, respectively. From the results, we found that the dewetting area increases when increasing annealing time. Moreover, the percentage of dewetting area of PS30K-ZnO1.0 is significantly lower than the other concentrations of the composite films and it is nearly constant after heating for a long time.

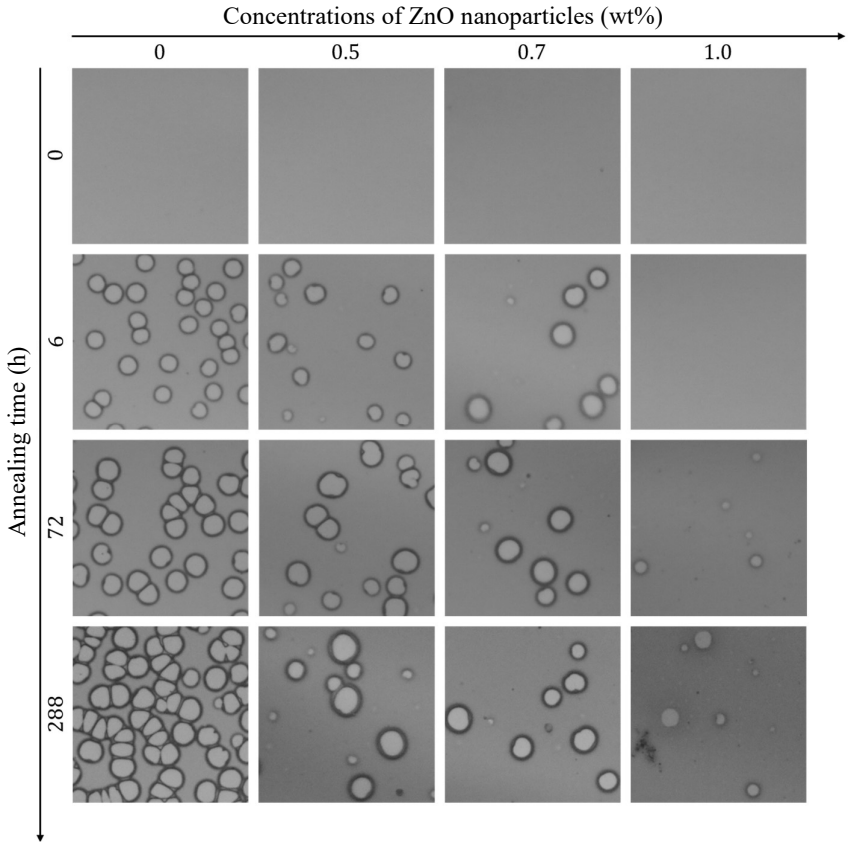

Figure 4. Optical microscope images of PS30K-ZnO films containing different concentrations of ZnO at 0, 0.5, 0.7, and 1.0 wt%, annealed temperature at 100°C for various time (magnification 1000X).

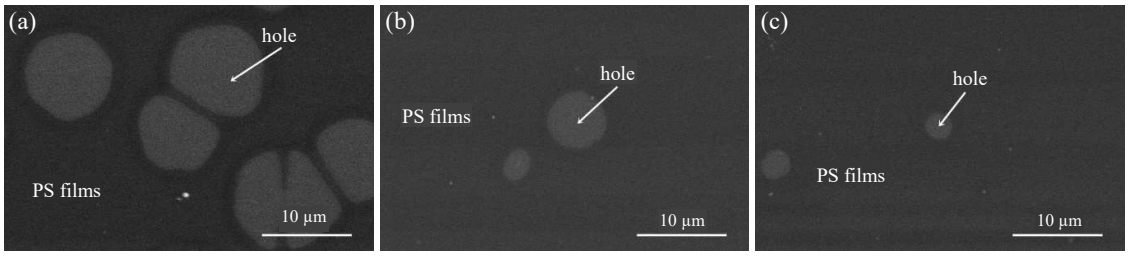

Figure 5. Scanning electron microscope images of PS30K-ZnO films, annealed temperature at 100°C for 72 h- (a) PS30K, (b) PS30K-ZnO0.7, and (c) PS30K-ZnO1.0 (magnification 10000X).

In addition, the slope of pure PS30K graph shows a higher slope which mean higher dewetting rate comparing with the composite films. For PS30K-ZnO0.5 and PS30K-ZnO0.7, the dewetting rate is high when annealing between 0-24 h and become slower between 24-288 h. Moreover, PS30K-ZnO1.0 film show the lowest slope, there is almost no dewetting rate after 24 h of heating, which indicate that addition of ZnO nanoparticles at 1.0 wt% strongly suppresses dewetting in PS30K film. The film has great thermal stability against dewetting. Therefore, PS30K-ZnO1.0 is the appropriate concentration for inhibition of dewetting behavior in PS30K films.

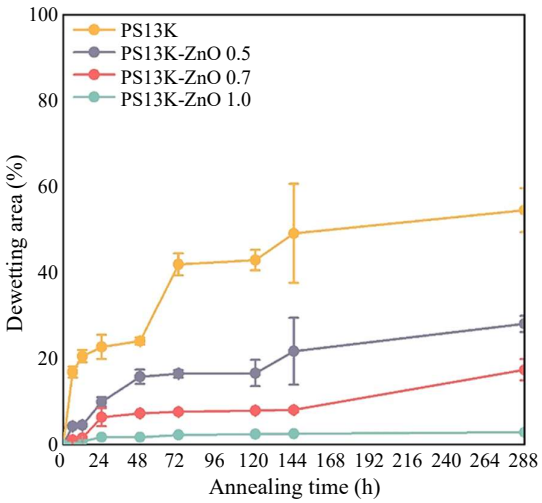

Figure 6. Graph show percentage of dewetting area and annealing time of PS30K-ZnO films with concentrations 0, 0.5, 0.7, and 1.0 wt%.

All results, OM images in Figure 4, SEM images in Figure 5, and percentage of dewetting area in Figure 6, exhibit the similarity. For PS30K system, the dewetting behavior occurs after annealing for 6 h and become intermediate stage of dewetting when annealing time is increased to 288 h. PS30K-ZnO0.5 and PS30K-ZnO0.7 films, show dewetting behavior after annealing for 6 h and slowly increase dewetting area when increasing annealing time to 24 h. PS30K-ZnO1.0 starts dewetting at 24 h of annealing and after that increasing annealing time cannot initiate further dewetting of this film. Addition of ZnO nanoparticles at 1.0 wt% in PS30K show a high performance to extend thermal stability of the PS30K system. The percentage of dewetting area of PS30K-ZnO1.0 films is constant at about 2% against heating for 288 h.

Comparing the dewetting behavior of PS13K and PS30K system, we found that addition of ZnO nanoparticles can raise thermal stability of the thin PS films. The optimum concentration of ZnO nanoparticles to inhibit dewetting are 0.7 and 1.0 wt% for PS13K and PS30K system, respectively. In addition, for both systems, the dewetting rate of PS-ZnO is less than of pure PS; however, there are a few differences between PS13K and PS30K. In PS13K, though the dewetting rate of composite film is slower than the pure PS, the trend of graph is rapidly increasing and can possibly reach to 100% of dewetting area if annealing time increased. In contrast, PS30K-ZnO films show no dewetting rate, and have a constant dewetting area after heating for 24 h till 288 h. It can be concluded that addition of ZnO nanoparticles can stop dewetting behavior in PS30K film system.

From Roy research, when surface energy of substrate is higher than surface energy of nanoparticles, at all concentrations, the nanoparticles tend to migrate to the interface between substrate and polymer film [19]. From literature reviews, the surface energy of ZnO is about 40-51 $mJ \cdot m^{-2}$ [30-32] and, in 2018, Narayan *et al.* [33] investigates that the surface energies of native oxides of Si wafer is 53 $mJ \cdot m^{-2}$. Therefore, in our system, we assume that ZnO nanoparticles migrate to the interface between PS film and Si substrate. Due to the obstruction of polymer matrix, ZnO nanoparticles will push down on polymer chain which according to our hypothesis, pinning contact line effect.

The shorten polymer chain, PS13K, is selected in this study to compare with our previous research [25]. The different of molecular weight indicate the length of the polymer chain which reflects entanglement and motion in the polymer film. Normally, the shorter length of the polymer chain shows less thermal stability because the polymer chain is short and easily move. While the higher molecular weight, long chain polymer, presents limited motion. Base on the pinning contact line effect, we assume that, the movement of PS chain will affect an ability of nanoparticle inhibition. Because of the difference in molecular weight, the shape of holes in PS13K and PS30K systems are different. Heating thin films at higher

temperature than T_g activates stress, then polymer matrix moves to merge and release stress in the film. For PS13K, short polymer chain and high mobility, the polymer chains which are pressed by ZnO nanoparticles, to release stress, they move and expand to the side of the nanoparticles. Therefore, the holes that occur in PS13K-ZnO films are flower-like shaped. On the other hand, for PS30K, long polymer chain and low mobility, they cannot move through the gap between nanoparticles. Hence the holes stop expand and the films create a new hole to release stress instead. Thus, the annealed PS30K-ZnO films exhibit small circular holes in every heating time condition.

3.3 Surface energies of PS13K-ZnO and PS30K-ZnO films

Surface energy is calculated by contact angle values from contact angle measurement. Two liquids, deionized water (DI water) and diiodomethane are dropped on the surface of PS13K-ZnO and PS30K-ZnO system. After that, the contact angles are measured between the surface of polymer thin film with DI water and the surface of polymer thin film with diiodomethane. The average contact angle of PS13K-ZnO and PS30K-ZnO films in each concentration is calculated by using Owens Wendt's equation [29].

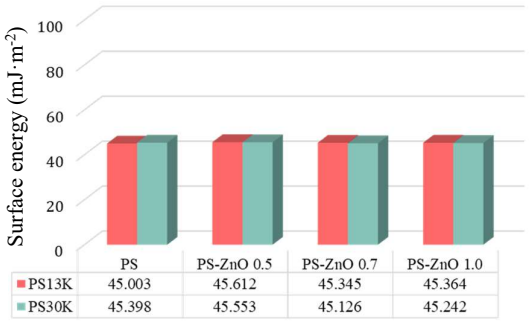

Figure 7. Surface energy of PS13K-ZnO and PS30K-ZnO composite films containing different concentrations of ZnO at 0, 0.5, 0.7, and 1.0 wt%.

The surface tensions of water (γ_{water} = 72.7, γ^d_{water} = 21.8 and γ^h_{water} = 50.9 mJ·m^{-2}) and diiodomethane ($\gamma_{diiodomethane}$ = $\gamma^d_{diiodomethane}$ = 50.0 and $\gamma^h_{diiodomethane}$ = 0 mJ·m^{-2}) are used to calculate in equation (1). Figure 7 shows the surface energies of PS13K-ZnO and PS30K-ZnO films in each concentration. From the results, we found that the surface energies of PS13K-ZnO at various concentrations of nanoparticles are similar, as same as in PS30K system, the result is not presented here. The surface energies of pure PS and PS-ZnO composite films indicate there is no difference in physical properties in the polymer matrix before and after adding ZnO nanoparticles [24-25]. Therefore, addition of ZnO nanoparticles does not affect the physical properties of both PS13K and PS30K systems. We can conclude that the mechanism to inhibit dewetting behavior of PS-ZnO film is not the change of composite film properties. The migration of ZnO nanoparticles to the PS-substrate film interface play an important role to suppress dewetting.

4. Conclusions

From the experiment, ZnO nanoparticles can be used as an additive for dewetting inhibition in both PS13K and PS30K matrix. The thermal stability of PS13K and PS30K are increased after addition of small amounts of ZnO nanoparticles. The concentrations of ZnO nanoparticles at 0.7 and 1.0 wt% are the appropriate concentration for dewetting suppression in PS13K and PS30K, respectively. However, addition of ZnO nanoparticles does not change the surface energies of the composite films. Therefore, the existence of ZnO in PS matrix does not affect physical properties. Moreover, the surface energies of Si substrate and ZnO can explain the migration of ZnO nanoparticles in polymer matrix. We conclude that the nanoparticles migrate to the substrate and press down on the polymer chain which refer to pinning contact line effect. We found that the difference in molecular weight of PS affects the dewetting pattern because the shapes of holes in PS13K-ZnO and PS30K-ZnO are different.

5. Acknowledgements

This research was funded by King Mongkut's University of Technology North Bangkok (KMUTNB). Contract no. KMUTNB-61-GOV-03-15. Our success in thin film research was supported by Dr. Kitiphat Sinthiptharakoon from National Nanotechnology Center (NANOTEC), National Science and Technology Development Agency (NSTDA). This research is partially supported by Scientific Instrument and High-Performance Computing Center (SICC), King Mongkut's University of Technology North Bangkok (KMUTNB) and NSTDA Characterization and Testing Service Center (NCTC), National Science and Technology Development Agency (NSTDA), for characterization tools.

References

[1] X. J. Cai, H. M. Yuan, A. Blencowe, G. G. Qiao, J. Genzer, and R. J. Spontak, "Film-stabilizing attributes of polymeric core-shell nanoparticles," *ASC Nano*, vol. 9, pp. 7940-7949, 2015.

[2] J. K. Bal, T. Beuvier, A. B. Unni, E. A. Chavez Panduro, G. Vignaud, N. Delorme, M. S. Chebil. Y. Grohens, and A. Gibaud, "Stability of polymer ultrathin films (<7 nm) made by a top-down approach," *ASC Nano*, vol. 9, pp. 8184-8193, 2015.

[3] D. A. Barkley, N. Jiang, M. Sen, M. K. Endoh, J. G. Ruidick, T. Koga, Y. Zhang, O. Gang, G. Yuan, S. K. Satija, D. Kawaguchi, K. Tanaka, and A. Karim, "Chain conformation near the buried interface in nanoparticle-stabilized polymer thin films," *Macromolecules*, vol. 50, pp. 7657-7665, 2017

[4] S. Lee, W. Lee, N. L. Yamada, K. Tanaka, J. H. Kim, H. Lee, and D. Y. Ryu, "Instability of polystyrene film and thermal behaviors mediated by unfavorable silicon oxide interlayer," *Macromolecules*, vol. 52, pp. 7524-7530, 2019.

[5] A. Alizadeh Pahlavanm L. Cueto-Felgueroso, A. E. Hosoi, G. H. McKinley, and R. Juanes, "Thin films in partial wetting: stability, dewetting and coarsening," *Journal of Fluid Mechanics*, vol. 845, pp. 642-681, 2018.

[6] M. Baglioni, C. Montis, F. Brandi, T. Guaragnone, I. Meazzini, P. Baglioni, and D. Berti, "Dewetting acrylic polymer films with water/propylene carbonate/surfactant Mixtures-Implications for cultural heritage conservation," *Physical Chemistry Chemical Physics*, vol. 19, pp. 23723-23732, 2017.

[7] R. Traiphol, "Influences of chain heterogeneity on instability of polymeric thin films: Dewetting of polystyrene, polychloromethylstyrene and its copolymers," *Journal of Colloid and Interface Science*, vol. 310, pp. 217-228, 2007.

[8] L. Xue and Y. Han, "Inhibition of dewetting of thin polymer films," *Progress in Materials Science*, vol. 57, pp. 947-979, 2012.

[9] P. Cao, P. Bai, A. A. Omrani, Y. Xiao, K. L. Meaker, H. Z. Tsai, A. Yan, H. S. Jung, R. Khajeh, G. F. Rodgers, Y. Kim, A. S. Aikawa, M. A. Kolaczkowski, Y. Liu, A. Zettl, K. Xu, M. F. Commie, and T. Xu, "Preventing thin film dewetting via graphene capping," *Advanced Materials*, vol. 29, pp. 1-6, 2017.

[10] T. Xia, Y. P. Qin, and T. Huang, "Phase Separation, Wetting and Dewetting in PS/ PVME blend thin films: dependence on film thickness and composition ratio," *Chinese Journal of Polymer Science*, vol. 36, pp. 1084-1092, 2018.

[11] T. Kato, Y. Liu, Y. Murai, M. Kubo, E. Shoji, T. Tsukada, S. Takami, and T. Adschiri, "Effect of surface modifier of nanoparticles on dewetting behaviors of polymer nanocomposite thin films," *Journal of Chemical Engineering of Japan*, vol. 51, pp. 282-288, 2018.

[12] S. Chandran, R. Handa, M. Kchaou, S. A. Akhrass, A. N Semenov, and G. Reiter, "Time allowed for equilibration quantifies the preparation induced nonequilibrium behavior of polymer films," *ACS Macro Letters*, vol. 6, pp. 1296-1300, 2017.

[13] G. T. Carroll, M. E. Sojka, X. Lei, N. J. Turro, and J. T. Koberstein, "Photoactive additives for cross-linking polymer films: inhibition of dewetting in thin polymer films," *Langmuir*, vol. 22, pp. 7748-7754, 2006.

[14] S. A. Akhrass, R. V. Ostaci, Y. Grohens, E. Drockenmuller and G. Reiter, "Influence of progressive cross-linking on dewetting of polystyrene thin films," *Langmuir*, vol. 24, pp. 1884-1890, 2008.

[15] M. Kubo, Y. Takahashi, T. Fuiji, Y. Liu, K. I. Sugioka, T. Tsukada, K. Minami, and T. Adschiri, "Thermal dewetting behavior of polystyrene composite thin films with organic-modified inorganic nanoparticles," *Langmuir*, vol. 30, pp. 8956-8964, 2014.

[16] N. Pangpaiboon, N. Traiphol, V. Promarak, and R. Traiphol, "Retradation the dewetting dynamics of ultrathin polystyrene films using highly branched aromatic molecules as additives," *Thin Solid Films*, vol. 548, pp. 323-330, 2013.

[17] N. Pangpaiboon, N. Traiphol, and R. Traiphol, "Enhancing the stability of polystyrene ultrathin films by using star-shape polymers as dewetting inbitors," *Journal of Coating Technology and Research*, vol. 12, pp. 1173-1183, 2015.

[18] Y. Liu, T. Kato, M. Kubo, K. I. Sugioka, T. Tsukada, S. Takami, and T. Adschiri, "Annealing-promoted unidirectional migration of organic-modified nanoparticles embedded two-dimensionally in polymer thin films," *Journal of Applied Polymer Science*, vol. 132, pp. 1-9, 2015.

[19] S. Roy, D. Bandyopadhyay, A. Karim, and R. Mukherjee, "Interplay of substrate surface energy and nanoparticle concentration in suppressing polymer thin film dewetting," *Macromolecules*, vol. 48, pp. 373-382, 2015.

[20] K. A. Barnes, A. Karim, J. F. Douglas, A. I. Nakatani, H. Gruell, and E. J. Amis, "Suppression of dewetting in nanoparticle-filled polymer films," *Macromolecules*, vol. 33, pp. 4177-4185, 2000.

[21] D. A. Barkley, N. Jiang, M. Sen, M. K. Endoh, J. G. Rudick, T. Koga, Y. Zhang, O. Gang, G. Yuan, S. K. Satija, D. Kawaguchi, K. Tanaka, and A. Karim, "Chain conformation near the buried interface in nanoparticle-stabilized polymer thin films," *Macromolecules*, vol. 50, pp. 7657-7665, 2017.

[22] N. Pangpaiboon and N. Traiphol, "Dewetting suppression of polystyrene thin films using titanium dioxide nanoparticles," *Key Engineering Materials*, vol. 608, pp. 218-223, 2014.

[23] N. Pangpaiboon, "Effects of zinc oxide nanoparticles on polystyrene thin films," *Journal of Science & Technology, Ubon Ratchathani University,* Special Issue, pp. 8-11, 2016.

[24] A. Wongtrakul, K. Watchana, and N. Pangpaiboon, "Thermal stability of zinc oxide polystyrene composite thin film," *The Journal of Applied Science*, vol. 16, pp. 82-86, 2017.

[25] J. Thapoung, K. Tasurin, N. Traiphol, and N. Pangpaiboon, "The effects of concentrations of ZnO nanoparticles on dewetting suppression of PS thin films," *Journal of Metal, Materials and Minerals*, vol. 28, pp. 89-93, 2018.

[26] A. Jayakumar, K. V. Heera, T. S. Sumi, M. Joseph, S. Mathew, G. Praveen, I. C. Nair, and E. K. Radhakrishnan, "Starch-PVA composite films with zinc-oxide nanoparticles and phytochemicals as intelligent pH sensing wraps for food packaging application," *International Journal of Biological Macromolecules*, vol. 136, pp. 395-403, 2019.

[27] S. Shankar, and J. W. Rhim, "Effect of types of zinc oxide nanoparticles on structural, mechanical and antibacterial properties of poly (lactide)/poly(butylene adipate-co-terephthalate) composite films," *Food Packaging and Shelf Life*, vol. 21, pp. 1-7, 2019.

[28] K. Rojas, D. Canales, N, Amigo, L. Montoille, A. Cament, L. M. Rivas. O. G. Castell, P. Reyes, M. T. Ulloa, A. R. Greus, and P. A. Zapata, "Effective antimicrobial materials based on low-density polyethylene (LDPE) with zinc oxide (ZnO) nanoparticles," *Composites Part B*, vol. 172, pp. 173-178, 2019.

[29] D. Y. Kwok and A.W. Neumann, "Contact angle measurement and contact angle interpretation," *Advances in Colloid and Interface Science*, vol. 81, pp. 167-249, 1999.

[30] L. D. Trino, L. F.G. Dias, L. G.S. Albano, E. S. Bronze-Uhle, E. C. Rangel, C. F.O. Graeff, and P. N. Lisboa-Filho, "Zinc oxide surface functionalization and related effects on corrosion resistance of titanium implants," *Ceramic International*, vol. 44, pp. 4000-4008, 2018.

[31] I. Torchinsky and G. Rosenman, "Wettability Modification of Nanomaterials by Low-Energy Electron Flux," *Nanoscale Res Lett*, vol. 4, pp. 21209-1217, 2009.

[32] J. Zhang, Y. Zhang, K. Tse, B. Deng, H. Xu, and J. Zhu, "New approaches for calculating absolute surface energies of wurtzite (0001)/ (0001): A study of ZnO and GaN," *Journal of Applied Physics*, vol. 119, pp. 1-8, 2016.

[33] S. R. Narayan, J. M. Day, H. L. Thinakaran, N. Herbots, M. E. Bertram, C. E. Cornejo, T. C. Diaz, K. L. Kavanagh, R. J. Culbertson, F. J. Ark, S. Ram, M. W. Mangus, and R. Islam, "Comparative study of surface energies of native oxides of Si(100) and Si(111) via three liquid contact angle analysis," *Materials Research Society*, vol. 3, no. 57-58, pp. 3379-3390, 2018.